Earth **Surface**
Dynamics
Discussions
EGU

Global analysis of short- versus long-term drainage basin erosion rates

Shiuan-An Chen[1], Katerina Michaelides[1,2,3], Michael Bliss Singer[3,4,5], David A. Richards[1,2]

[1]School of Geographical Sciences, University of Bristol, Bristol, BS8 1SS, UK
5 [2]Cabot Institute for the Environment, University of Bristol, Bristol, UK
[3]Earth Research Institute, University of California Santa Barbara, Santa Barbara, California 91306, USA
[4]School of Earth and Environmental Sciences, Cardiff University, Cardiff, CF10 3AT, UK
[5]Water Research Institute, Cardiff University, Cardiff, CF10 3AX, UK

Correspondence to: Shiuan-An Chen (sc16970@bristol.ac.uk)

10 **Abstract.** Measuring erosion rates, analysing their temporal variations, and exploring environmental controls are crucial in the field of geomorphology because erosion through sediment transport in drainage basins shapes landforms and landscapes. Thus, important insights into landscape controls can be gleaned from analyses of erosion rates measured over different timescales. Suspended sediment flux and in situ cosmogenic radionuclides have been widely used for estimating short- and long-term erosion rates of drainage basins, respectively. Even though analyses of erosion rates have been conducted across

15 the globe, there are still gaps in understanding of the links between environmental controls and erosion rates between timescales, especially the influence of climate, which is complex and covaries with other factors. To begin unpicking controls on landscape evolution across the globe, we compiled short- and long-term erosion rates (estimated from suspended sediment yield and in situ beryllium-10, ^{10}Be, respectively) and analysed their relationships with climate, topography, and anthropogenic activity. The results show that: 1) A non-linear relationship exists between aridity and long-term erosion rates,

20 resulting from the balance between precipitation and vegetation cover; 2) Long-term erosion rates are higher in mid- and high-latitude regions with high humidity, reflecting glacial processes during ice ages; 3) Long-term erosion rates are positively related to the steepness of drainage basins, showing that both climate and topography are the common factors; 4) Human activities increase short-term erosion rates which outweigh natural controls; and 5) The ratios of short- to long-term erosion rates are negatively related to basin area, reflecting the buffering capacity of large basins. These results highlight the

25 complex interplay of controlling factors on land surface processes and reinforce the view that timescale of observation reveals different erosion rates and principal controls.

1 Introduction

The erosion rate of a drainage basin is an important geomorphic quantity because it reflects the net flux of sediment from source to sink in drainage basin and correspondingly, the rate and spatial pattern of landscape evolution. Despite impressive

30 and increasing collections of long- and short-term erosion rates for drainage basins across the globe, it remains equivocal

whether there are identifiable patterns in these erosion rates that reflect the prevailing climatic regime and/or anthropogenic activities within basins.

Suspended sediment flux records, typically measured over annual to decadal timescales in the recent past, describe the
35   history of fine sediment transport from uplands to lowlands within riverine flow (Milliman and Meade, 1983). In situ cosmogenic radionuclide concentrations within riverine sediment can be used to estimate basin-averaged exposure ages for timescale of tens of thousands years or more, integrating long-term erosion and deposition signals (Granger and Schaller, 2014; von Blanckenburg and Willenbring, 2014). These two proxies for basin-wide erosion are commonly used independently in geomorphology to investigate spatial and temporal changes in erosion in response to climatic and tectonic
40   forcing (Clapp et al., 2001; Pan et al., 2010; Wittmann et al., 2011; Yizhou et al., 2014) and to compare erosions rates between basins (Milliman and Meade, 1983; Milliman and Syvitski, 1992; Summerfield and Hulton, 1994; Dedkov and Mozzherin, 1996; Portenga and Bierman, 2011; Harel et al., 2016). The combination of these proxies enables the investigation of potential drivers of erosion and consideration of the role of time averaging on erosion rates (Kirchner et al., 2001; Schaller et al., 2001; Covault et al., 2013). To quantify the pattern of erosion rates and the dominant controls on
45   erosion rates at different timescales at the global scale, we compiled drainage basin erosion rates estimated from suspended sediment yield (short-term) and cosmogenic nuclides (long-term) from several global databases. We then compared short- and long-term rates across the globe, classified by climate and anthropogenic activity, to explore the linkages between erosion and its primary drivers over different timescales.

50   Erosion rates based on suspended sediment yield are calculated by measuring the sediment concentration and discharge at a gauging station over years to decades, and then converting their product into mean annual sediment flux, then to sediment yield (t ha^{-1} yr^{-1}) normalised by upstream drainage area, and subsequently to erosion rate (mm yr^{-1}), assuming a basin-averaged soil bulk density. This method provides an averaged value of erosion rate for the upstream area that neglects the storage of sediment during transportation and assumes that eroded sediments are all transported as suspended load. This is a
55   reasonable approximation because 1) storage of sediment can be considered to be negligible over longer timescales, and 2) suspended load dominates sediment flux (> 90%) for the majority of drainage basins, except high relief or dryland catchments (Milliman and Meade, 1983; Dedkov and Mozzherin, 1996; Singer and Dunne, 2004; Milliman and Syvitski, 1992; Laronne, 1993; Tooth, 2000; Singer and Michaelides, 2014). Suspended sediment records provide a record of recent and potentially transient responses within landscapes to climatic and/or anthropogenic forcing (Walling and Webb, 1996;
60   Walling and Fang, 2003).

In situ cosmogenic radionuclides are a common tool for estimating erosion rates based on exposure age dating at timescales from 10^3 to 10^5 yr. In situ cosmogenic radionuclides are produced by the interaction of cosmic rays with minerals in rocks and soils in the uppermost few metres of the Earth's surface. The concentration of cosmogenic radionuclides near the surface

Earth Surface
Dynamics
Discussions
EGU

65   is principally a function of the production rate, radioactive decay rate and erosion rate (or rate of surface stripping). Therefore, cosmogenic exposure age dates can be used for estimating drainage basin erosion rates (Brown et al., 1995; Granger et al., 1996; Granger et al., 2013; Granger and Schaller, 2014; von Blanckenburg and Willenbring, 2014). This method, when applied to riverine sediments, also provides averaged erosion rate, assuming no sediment storage within the upstream basin. Furthermore, this method assumes that: erosion rate is faster than the radioactive decay rate (for [10]Be,

70   erosion rate should be faster than 0.3 mm kyr^{-1}); radionuclide concentration has achieved the balance between production, erosion and decay rates (the landscape is in a state of equilibrium); the nuclide concentration has no dependency on grain size (a narrow range of grain sizes is typically used for analysis); there is no erosion–deposition cycle in the drainage basin; and quartz exists in sediments throughout the entire basin (Brown et al., 1995; Granger et al., 2013; Dosseto and Schaller, 2016; Struck et al., 2018). Erosion rates estimated using cosmogenic nuclides represent longer timescales than suspended

75   sediment records (10^3–10^5 yr versus 10^0–10^1 yr), and are therefore suitable for analysing the influences of climate and tectonics, and insensitive to the influences of anthropogenic activities or recent stochastic events (Brown et al., 1995; von Blanckenburg, 2006; Granger et al., 2013; Granger and Schaller, 2014; Dosseto and Schaller, 2016).

         At both regional and global scales, suspended sediment yields and cosmogenic nuclides have been widely used for analysing

80   short- and long-term erosion rates, respectively. Suspended sediment analysis has been employed for many decades, initiated by major investment in a nationwide monitoring programmes (e.g. USGS) and subsequently replicated in many other countries. Exploration of the valuable data provided by programmes has revealed insights into the relationships between climatic and anthropogenic drivers and sediment yields. For example, Langbein and Schumm (1958) used a limited dataset on sediment yields to identify a non-linear relationship between sediment yields and effective mean annual precipitation

85   (MAP) across various biomes in the USA, with a peak in the semi-arid rainfall regimes. They considered both precipitation and vegetation cover to play important roles. Specifically, they suggested that at low MAP, there is also little vegetation, so erosion increases commensurately with rainfall via Hortonian overland flow. However, with sufficient rainfall, vegetation cover may increase and slow erosion rate because of increased interception, higher infiltration, and correspondingly higher evapotranspiration or subsurface storm flow (Dunne and Leopold, 1978). Thus, humid regions have lower sediment yields

90   than semi-arid landscapes. Subsequently, Walling and Kleo (1979) extended this analysis to include data from around the globe and therefore including regions with higher MAP than the USA. Their results show that for basins smaller than 10,000 km^2, sediment yield peaks in semi-arid regions, but also in Mediterranean and tropical monsoon climate zones, with a strong seasonal rainfall pattern and intense precipitation that can exceed the protection capacity of vegetation cover. In addition to climatic controls, land surface processes are strongly influenced by anthropogenic activities through construction, mining,

95   timber harvesting, and conversion of natural vegetation to agriculture (crop and pasture), the last of which is the most dominant in terms of area (Hooke, 2000). Global analyses of short-term erosion rates from suspended sediment records suggest that a change to agricultural land cover has enhanced erosion rates by one to two orders of magnitude (Dedkov and Mozzherin, 1996; Montgomery, 2007; Wilkinson and McElroy, 2007; Kemp et al., 2020).

100 Regarding long-term erosion rates, a non-linear relationship between MAP and erosion rate was developed by (Mishra et al., 2019) on the basis of a global compilation of ^{10}Be measurements (n = 1,790). Whilst significant scatter is observed in the data, they identify a general increase in erosion rate to a local maximum MAP at ~ 1,000 mm, followed by a slight reduction up to MAP of ~ 2,200 mm and then return to increasing values for higher MAP. The relationship is explained by the interrelated influences of precipitation and vegetation cover as suggested for short-term studies (e.g. Langbein and Schumm,

105 1958), although their pattern of erosion rate change with MAP is quite different.

In addition to these climate/vegetation controls, glaciers and wildfires exert important influences on long-term erosion rates. Glaciers shape the land surface directly through the stripping of rock underneath basal ice, and through freeze–thaw and weathering processes on the margins of ice (Harel et al., 2016; Cook et al., 2020). Glacial erosion, for example, has been

110 shown to increase long-term erosion rates in temperate and cold regions, especially within mid- and high-latitudes (Portenga and Bierman, 2011; Harel et al., 2016). Wildfires, on the other hand, are more prevalent during dry periods and the occurrence is modified by variation of temperature and wind regimes (Pierce et al., 2004; Han et al., 2020). Wildfires burn the vegetation cover and deposit loose material on the hillslope, destroy root system underground, decrease the infiltration rate, and provide the material for transportation (Cannon et al., 1998; Pierce et al., 2004). Burned areas are more susceptible

115 to debris flow and landslides, which transports sediments from hillslopes to river channels, and increase the erosion rate of drainage basins over longer timescales (Cannon et al., 1998; Meyer et al., 2001).

Topography, tectonics, and lithology also influence erosion rates. For example, erosion rates tend to be positively related to total basin relief and slope gradient, tectonic uplift rates, and the erodibility of lithology, for short-term (Milliman and Meade,

120 1983; Milliman and Syvitski, 1992; Summerfield and Hulton, 1994; Aalto et al., 2006; Syvitski and Milliman, 2007; Milliman and Farnsworth, 2011; Yizhou et al., 2014) and long-term erosion rates (Granger et al., 1996; Bierman and Caffee, 2001; Schaller et al., 2001; von Blanckenburg, 2006; Binnie et al., 2007; DiBiase et al., 2010; Portenga and Bierman, 2011; Wittmann et al., 2011; Covault et al., 2013; Codilean et al., 2014; Harel et al., 2016; Schmidt et al., 2016; Grin et al., 2018; Struck et al., 2018; Tofelde et al., 2018; Hilley et al., 2019). However, many of these physiographic controls are not

125 independent and hamper efforts to deconvolve their relative influence (Milliman and Farnsworth, 2011). For example, a basin with rapid tectonic uplift tends to have both higher relief and gradients and lower rock strength due to the high density of faults and joints (Binnie et al., 2007; Grin et al., 2018). Furthermore, rapidly uplifting mountain ranges are subject to significant orographic precipitation (e.g. Himalayas, Taiwan), making it challenging to distinguish between the tectonics or climate forcing of erosion rates.

130

This study aims to understand the geographic expression of long- and short-term erosion rates around the globe and explore the climatic and other potential controls on erosion rates across spatial and temporal scales. We specifically address the

following questions: 1) What is the overall pattern of long- and short-term erosion rates across climate regimes? 2) To what extent do long-term erosion rates reflect glacial processes in mid- and high-latitude regions? 3) Is the previously observed non-linear relationship between precipitation and erosion rate applicable to both short and long timescales? 4) Do human activities outweigh other controls over short-term erosion rates? 5) How do basin topography and topology affect erosion rates?

To answer these questions, we compiled drainage basin erosion rates estimated from in situ ^{10}Be data (long-term) and suspended sediment yields from gauging stations (short-term). We then stratified the erosion rates using two commonly used climate classifications, Köppen–Geiger and Aridity Index, and analysed the relationships between erosion rates and potential controls, including climate, topography, and anthropogenic activity. We compared erosion rates around the globe with and without these controls to quantitatively assess their influence on erosion rates between timescales.

2 Methods

We compiled long- and short-term drainage basin erosion rates from existing databases and published literature. All data were stratified by the Köppen–Geiger climate classification and Aridity Index classification to examine relationships with climate. We also used ice extent at the last glacial maximum (LGM; Ray and Adams, 2001), MAP for the USA (calculated from CPC US Unified Precipitation data), mean slope gradient and total relief of river channels (extracted and calculated from Global Longitudinal Profiles database, GLoPro; Chen et al., 2019), and global agricultural regions (Foley et al., 2005).

Long-term erosion rates were obtained from the Open Cosmogenic Isotope and Luminescence Database (OCTOPUS), which includes basin-averaged erosion rates derived from cosmogenic nuclides (^{10}Be and ^{26}Al) and luminescence measurements in fluvial sediments (Codilean et al., 2018). This database classifies data based on the methods, regions, and degree of completeness. To gain the highest reliability and consistency, we only included ^{10}Be-derived erosion rates of CRN (cosmogenic radionuclide) International and CRN Australia categories from the database, resulting in a total of 3,074 data points (Fig. 1). For each data point, we extracted the erosion rate, coordinates, and drainage basin area.
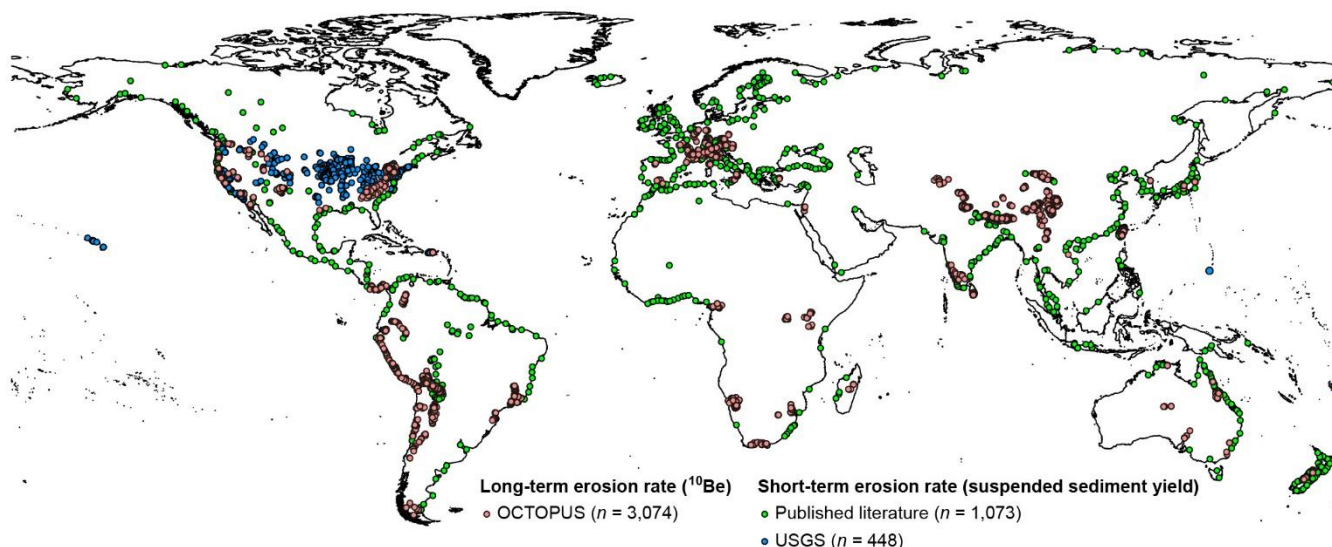
Figure 1: Global map of drainage basin erosion rate locations. Long-term erosion rates were obtained from OCTOPUS (Open Cosmogenic Isotope and Luminescence Database, red), estimated by [10]Be in the fluvial sediments. Short-term erosion rates were compiled from published literature (green) and USGS (blue), determined by suspended sediment yield of gauging stations. Coastline is from Nature Earth (https://www.naturalearthdata.com) in the Pseudo Plate Carree map projection.

Short-term erosion rates were compiled from the published literature and the USGS (National Water Information System, https://waterdata.usgs.gov/nwis), based on estimations from suspended sediment yields at gauging stations. From the published literature, we compiled sediment yields (t ha^{-1} y^{-1}) or erosion rates (mm ky^{-1}) at each data point. To convert erosion rates from sediment yields, we assumed sediment density to be 1.6 g cm^{-3} (= 1.6 t m^{-3}). Using this density, sediments with the depth of 0.1 mm across 1 ha area weight 1.6 t. A sediment yield of 1 t ha^{-1} y^{-1}, for example, is equivalent to an erosion rate of 0.0625 mm y^{-1} (or 62.5 mm ky^{-1}). If the coordinates of the gauging stations were not provided, we acquired the point coordinates from Google Maps. If data from the same gauging station were reported in multiple literature sources, we only included the erosion rate with the most recent data record. For the USGS data, two criteria were set for choosing gauging station data: 1) the monitoring time period needed to be > 5 years, and 2) the basin area < 2,500 km^2 (to avoid basins representing more than one climate zone). Note that some of the gauging stations meeting these criteria may be on the same river. We extracted the daily sediment discharge (t d^{-1}), converted this into sediment yield (t ha^{-1} y^{-1}) by summing the daily data and dividing by the number of years and basin area. The sediment yield was then converted into an erosion rate. In total, we obtained 1,521 short-term erosion rates; 1,073 from the published literature and 448 from USGS (Fig. 1), with corresponding station coordinates and drainage basin areas (Supplement).

The Köppen–Geiger (K–G) climate classification is based on biome types, defined by temperature and precipitation thresholds. Here we adopt the most updated version of Köppen–Geiger (Peel et al., 2007). The original classification

6

includes five main zones (Tropical, Arid, Temperature, Cold, and Polar) and 29 sub-zones. We classified data on the basis of the main Köppen–Geiger zones to provide sufficient data points in each category, and we excluded Polar because there are too few data. The Aridity Index (AI) is a quantitative metric for representing water balance and is calculated by dividing MAP by mean annual potential evapotranspiration from the Global Aridity and PET Database (Trabucco and Zomer, 2009).

185 For ease of statistical comparison, we have adopted a categorical approach and use the following thresholds for the Aridity Index: Hyper-arid (< 0.03), Arid (0.03–0.2), Semi-arid (0.2–0.5), Dry sub-humid (0.5–0.65), and Humid (> 0.65).

There are numerous environmental controls on erosion rates around the globe, among them glacial processes during the ice ages (Portenga and Bierman, 2011; Harel et al., 2016), topography (e.g. Portenga and Bierman, 2011), and human activities

190 (e.g. Covault et al., 2013). To explore the influence on erosion rates of these three broad drivers, we considered the extent of ice coverage at the LGM, the slope gradient and relief of river channels, and the spatial pattern of agricultural regions. Previous studies typically used MAP to examine climatic controls on erosion rates (e.g. Langbein and Schumm, 1958; Walling and Kleo, 1979). Thus, in addition to classifying erosion rates by climate zones, we also used MAP across the continental USA for further analysis.

195

The extent of glacial processes at the ice ages was determined from Ray and Adams (2001), which provides the global vegetation map at the LGM (25,000–15,000 BP) based on fossil and sedimentary information, and expert consultation. Since the timescale of [10]Be-derived erosion rates is in the range of 10^3–10^5 years, the data cover several ice ages. However, we used coverage of the last ice age as the most reliable estimate of glacial influences. The glacial regions at the LGM were

200 defined as the following five categories in the data source: Tundra, Steppe-tundra, Polar and alpine desert, Alpine tundra, and Ice sheet and other permanent ice.

The topographic parameters used here include the mean slope gradient and total relief of river longitudinal profiles extracted from the GLoPro database (Chen et al., 2019). GLoPro includes river longitudinal profiles around the globe which were

205 extracted from NASA's 30 m Shuttle Radar Topography Mission Digital Elevation Model (SRTM–DEM). The rivers in the database are the mainstem rivers (the longest rivers) of basins or sub-basins that do not cross Köppen–Geiger climate sub-zones. The recorded topographic data include the concavity, elevation, flow distance, and drainage area of each river profile. To extract river profiles from the database for comparing topographic parameters with erosion rates, we chose a subjective distance threshold as 150 m between river profiles and erosion rate sampling points (i.e. selecting river profiles which are

210 within 150 m to the closest erosion rate points), and calculated the mean slope gradient and total relief of river longitudinal profiles.

Anthropogenically impacted regions were determined from Foley et al. (2005), which provides global maps of croplands, and pastures and rangelands classified by the relative percentages of areas within these land uses. These maps were modified

215 from previous studies (Ramankutty and Foley, 1999; Asner et al., 2004), in which they classified land use types from satellite images using GIS analysis. We conservatively defined anthropogenic regions with higher than 50% area of croplands or pastures and rangelands.

MAP across the continental USA was obtained from CPC US Unified Precipitation data (https://www.esrl.noaa.gov/psd)
220 produced by National Oceanic and Atmospheric Administration Physical Sciences Laboratory (NOAA PSL). The data is in raster format with 0.25-degree resolution (~ 28 km at the equator), including daily precipitation rates from 1948 to 2006 (59 years). We summed the daily data of each grid in each year to convert daily data into yearly data and calculated the precipitation rates for all locations where we have erosion rates.

225 To analyse the statistical difference of erosion rates between climate zones, timescales, and environmental controls, we conducted the Kruskal–Wallis nonparametric hypothesis test by the built-in function, kruskalwallis, in MATLAB R2018a.

3 Results

3.1 Climate influence on long- and short-term erosion rates

Using both Köppen–Geiger and Aridity Index climate classifications, short-term erosion rates are significantly higher ($P <$
230 0.05) than long-term rates in all climate zones, except for the Cold K–G zone (Fig. 2, Table 1a). Within the Aridity Index categories, there is a general pattern of an increasing difference between long- and short-term erosion rates with higher aridity. However, these differences are only significant for the Arid and Semi-arid categories ($P < 0.05$, Fig. 2b, Table 1b).

For the long-term erosion rates, Tropical and Arid K–G zones have significantly ($P < 0.01$) lower erosion rates (medians =
235 29.7 and 32.2 mm kyr^{-1}, respectively) than Temperate and Cold zones (medians = 92.9 and 92.5 mm kyr^{-1}, respectively, Fig. 2a, Table 1a). Within the Aridity Index categories, long-term erosion rates are significantly lower in the dryland regions (i.e. Hyper-arid, Arid, and Semi-arid group of categories) compared to the non-dryland regions (i.e. Dry sub-humid and Humid group of categories, $P < 0.01$) (Fig. 2b), and there are no differences within them ($P > 0.05$, Table 1b). The maximum long-term erosion rates are exhibited in the Temperate and Cold K–G categories and in the Dry sub-humid AI category.
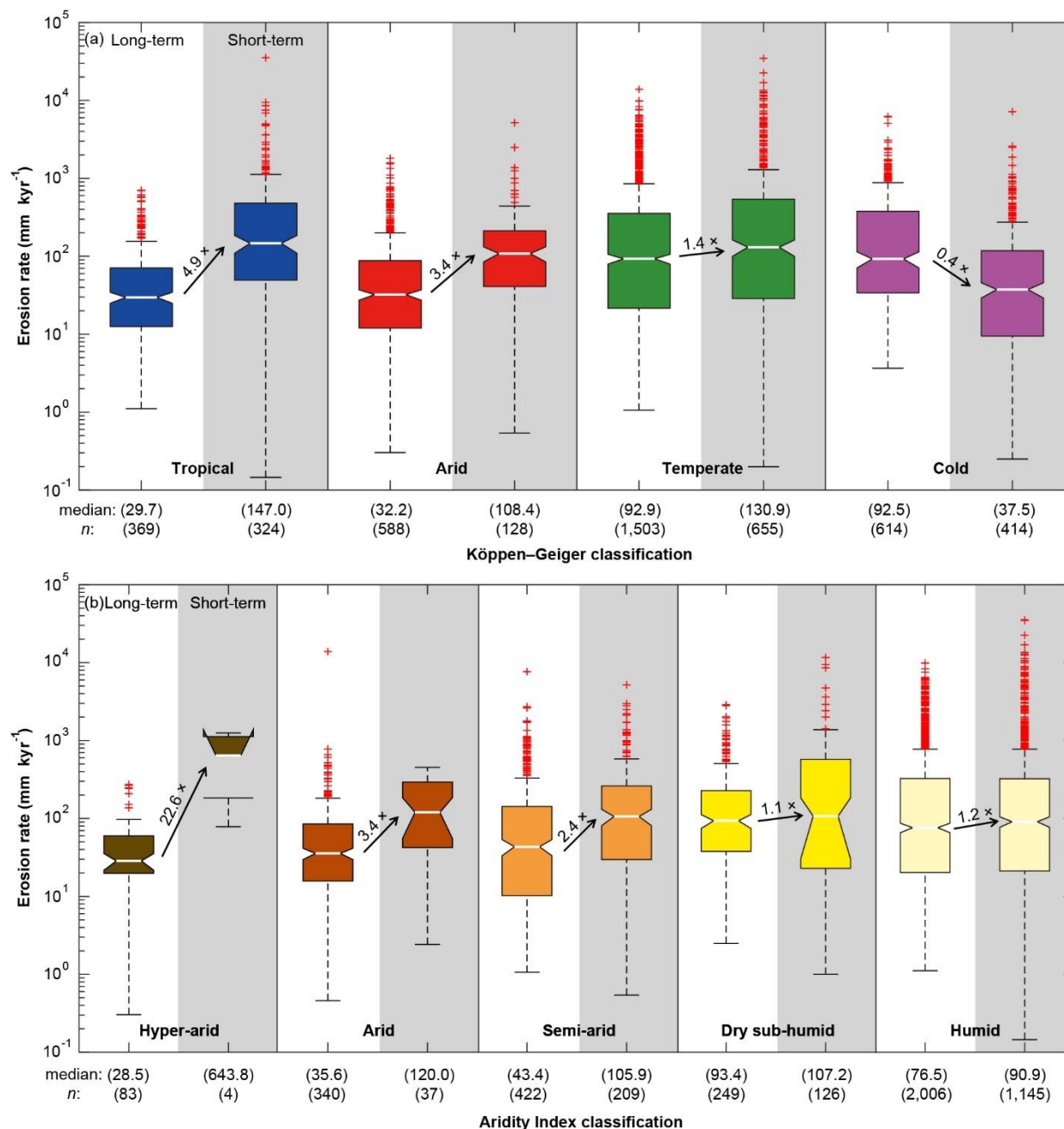
240

Figure 2: Long- and short-term erosion rates for climate zones of Köppen–Geiger climate classification (a) and Aridity Index classification (b). Boxplots with white backgrounds are the long-term rates, whilst the grey backgrounds are the short-term rates. On each box, the central line indicates the median value, and the bottom and top edges indicate the 25th and 75th percentiles, respectively. The notch represents the range of the median at the 5% significant level (note that the lower notch of short-term erosion rates of Hyper-arid category extends beyond the range of y-axis due to the limited number of samples in this category). The red crosses are the outliers. The arrow and number between boxplots in each climate zone indicate the trend and ratio of median values of short- to long-term rates ($R_{S/L}$). Median value and the number of data for each distribution are listed below.

245

250 **Table 1: The *P*-values of Kruskal–Wallis hypothesis testing of long-term (*n* = 3,074) and short-term (*n* = 1,521) erosion rates between climate zones of Köppen–Geiger climate classification (a) and Aridity Index classification (b), and between long- and short-term erosion rates of each climate zone. Bold numbers indicate *P*-values < 0.05. The number of data points for each climate zone is listed in Fig. 2.**

(a)

Long-term rates comparison				Short-term rates comparison			
	Arid	Temperate	Cold		Arid	Temperate	Cold
Tropical	0.88	**<0.001**	**<0.001**	Tropical	0.42	0.95	**<0.001**
Arid		**<0.001**	**<0.001**	Arid		0.82	**<0.001**
Temperate			0.54	Temperate			**<0.001**

Long- and short-term rates comparison	
Tropical	**<0.001**
Arid	**<0.001**
Temperate	**0.02**
Cold	**<0.001**

(b)

Long-term rates comparison					Short-term rates comparison			
	Arid	Semi-arid	Dry sub-humid	Humid		Arid	Semi-arid	Dry sub-humid	Humid
Hyper-arid	0.97	0.40	**<0.001**	**<0.001**	Hyper-arid	0.88	0.79	0.88	0.73
Arid		0.75	**<0.001**	**<0.001**	Arid		1	1	1
Semi-arid			**<0.001**	**<0.001**	Semi-arid			1	1
Dry sub-humid				0.53	Dry sub-humid				0.95

Long- and short-term rates comparison	
Hyper-arid	0.07
Arid	**0.02**
Semi-arid	**<0.001**
Dry sub-humid	1
Humid	1

255

To make our analysis comparable to other studies, we also analysed long-term erosion rates against MAP for all data points within the continental USA. The result shows a similar pattern of erosion rates as those analysed by Aridity Index, with the

highest erosion rates exhibited in the Dry sub-humid category (MAP ~ 600 mm, Fig. 3a) but also followed by a dip around

1,250 mm and a subsequent increase again in erosion rates in extremely humid regions, where MAP is higher than 1,300 mm.
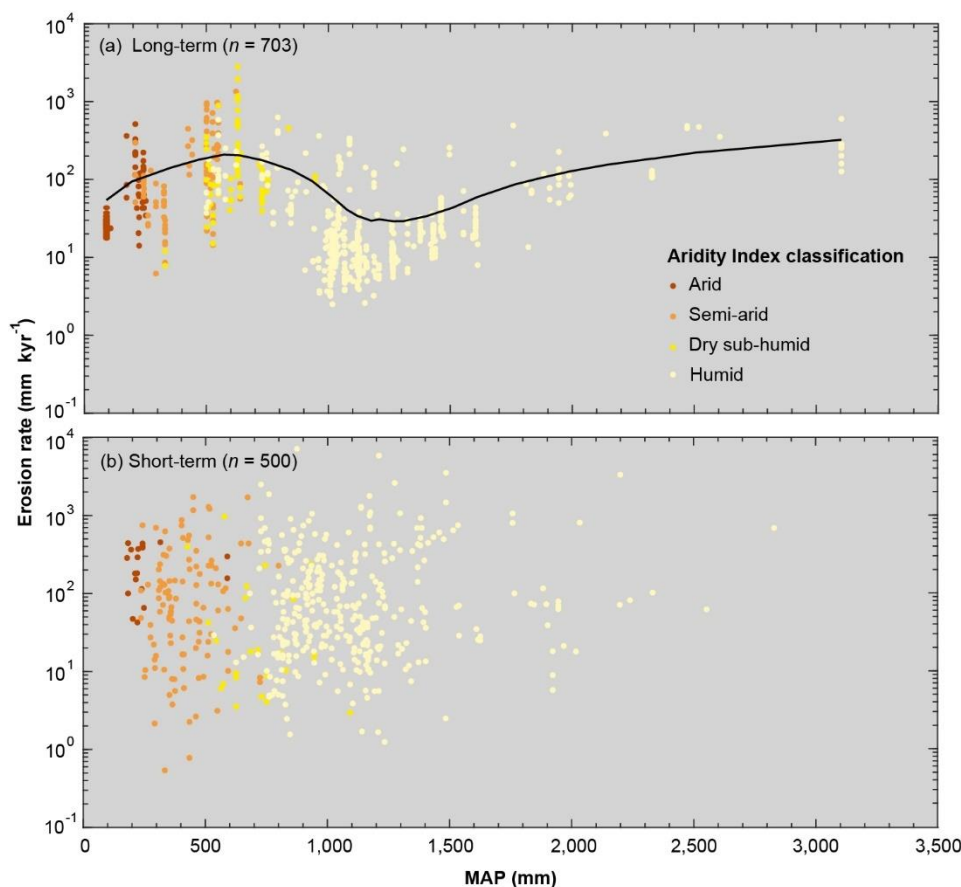
260

Figure 3: The relationships between mean annual precipitation (MAP) and long- (a) and short-term (b) erosion rates in the USA. The precipitation data were acquired from CPC US Unified Precipitation data. Points are colour coded by Aridity Index categories. Black curve in panel a is LOWESS regression, showing that long-term erosion rates peak at regions with precipitation about 600 mm and more than 1,300 mm. In contrast, no clear pattern is indicated for short-term erosion rates.

265

Within the short-term erosion rates, there is no dependency on climate according to either climate classifications ($P > 0.05$),

except in the Cold zone of K–G classification, where there were significantly lower erosion rates compared to other climate

zones ($P < 0.01$, Fig. 2a, b, Table 1). The medians of short-term erosion rates in all climates are generally between 90 and

270 150 mm kyr^{-1}, whereas the Cold K–G zone is only 37.5 mm kyr^{-1}, and the Hyper-arid AI category is as high as 643.8 mm

kyr^{-1} (note that the result of Hyper-arid category may not be robust because of limited available data). Similarly, there is no

apparent relationship between short-term erosion rates and MAP across the continental USA (Fig. 3b).

3.2 Influence of glaciation on long-term erosion rates

To explore the influence of past glaciations on long-term erosion rates, we compared data for those locations that are
275   currently in the Temperate K–G zone and were previously in glacial and pro-glacial zones during the Pleistocene (e.g. north-
western Europe, part of the Andes, the Himalayas, and New Zealand) against the Temperate sites that were not glaciated (Fig.
4). We find that long-term erosion rates for formerly glaciated regions of the Temperature zone are approximately 5 times
higher than in non-glaciated regions (medians = 202.3 and 41.4 mm kyr^{-1}, respectively, $P < 0.01$). This result accentuates the
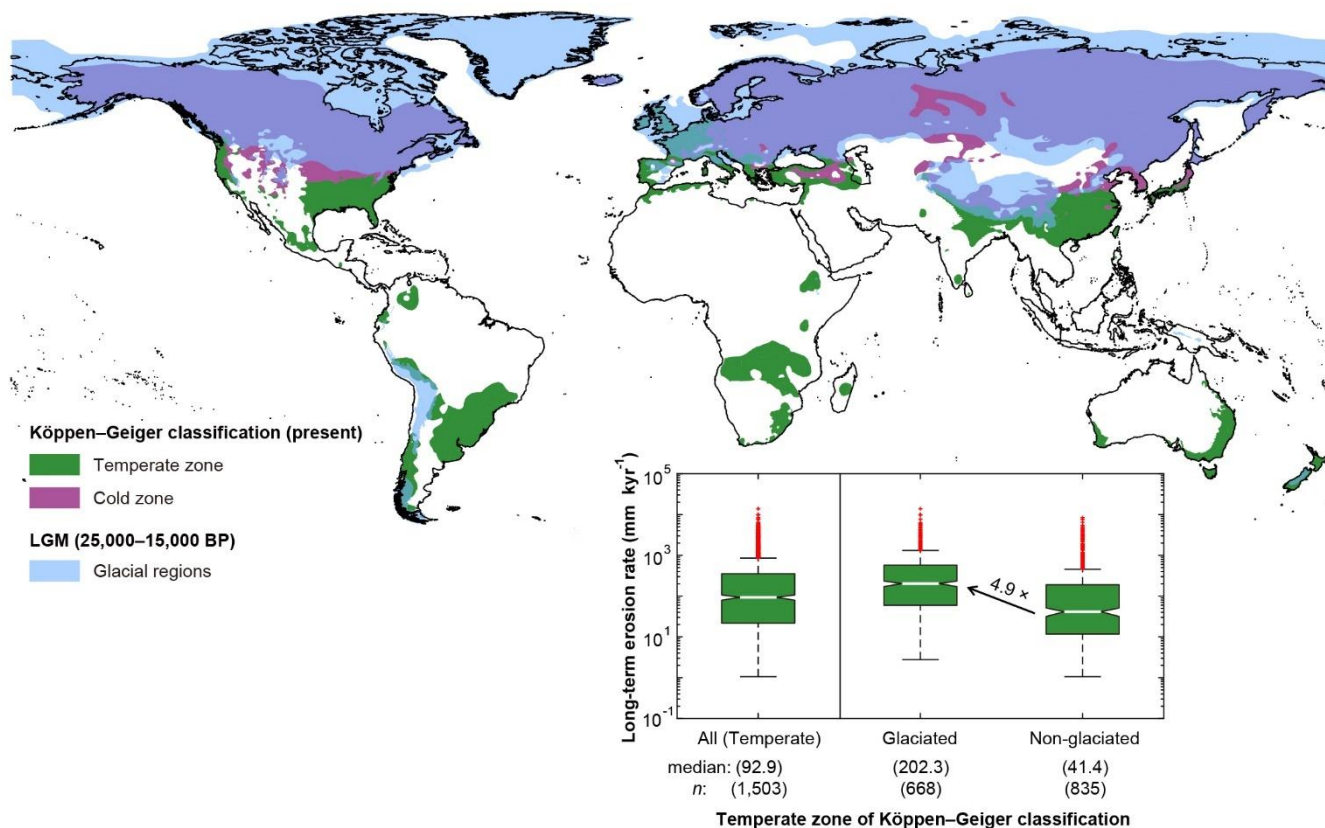role of glaciers in stripping surfaces across the landscape resulting in higher long-term erosion rates.

280

**Figure 4: The extent of glacial regions at the last glacial maximum (LGM) and the area of Temperate and Cold zones of Köppen–
Geiger climate classification in the present. The glacial regions were drawn from Ray and Adams (2001). The inserted figure**
285   **compares long-term erosion rates in the Temperate zone with and without glacial influences at the LGM. The figure shows 4.9
times higher median erosion rates in formerly glaciated regions compared to non-glaciated regions.**

3.3 Anthropogenic influences on short-term erosion rates

To examine the anthropogenic influences on short-term erosion rates, we compared the erosion rates in "croplands", and "pastures and rangelands", with erosion rates in regions with no such evidence of anthropogenic disturbance. Short-term

290 erosion rates in "croplands", and "pastures and rangelands" are 1.4 times higher than regions without these anthropogenic influences (78.3 mm kyr^{-1}, $P < 0.05$, Fig. 5). However, there was no significant difference in erosion rates between these anthropogenically impacted land use types (104.2 and 114.0 mm kyr^{-1}, respectively, $P > 0.05$).

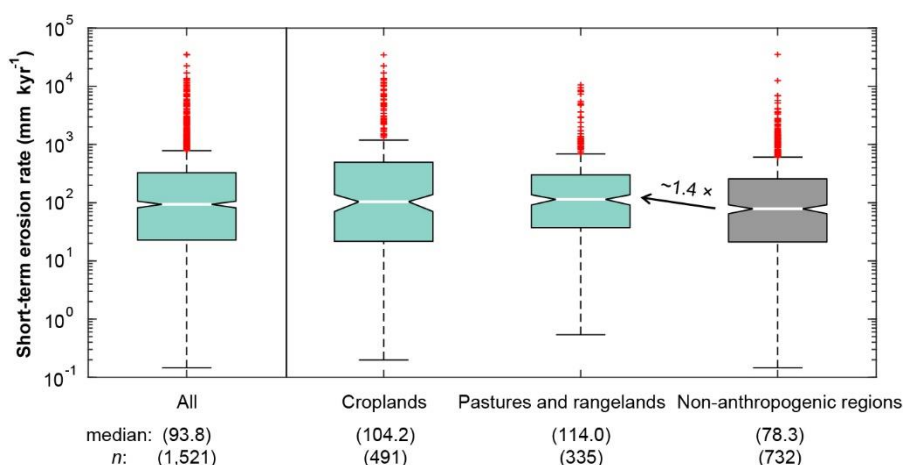|	median:	n:
All	(93.8)	(1,521)
Croplands	(104.2)	(491)
Pastures and rangelands	(114.0)	(335)
Non-anthropogenic regions	(78.3)	(732)

295 **Figure 5: The comparison of global short-term erosion rates with and without anthropogenic influences. The extent of "croplands" and "pastures and rangelands" were digitised from Foley et al. (2005). The figures show that short-term erosion rates with anthropogenic influences are about 1.4 times higher than in non-anthropogenic regions.**

3.4 Influence of basin characteristics

300 Finally, we explored the influences of spatial scale and topography on erosion rates. Across the whole datasets, for both long- and short-term erosion rates, there is no clear relationship with basin area (Fig. 6). To investigate this further, we grouped the erosion rates in three bins of basin area, < 500 km^2, 500–2,500 km^2, and $\geq 2,500$ km^2. The area thresholds were chosen to achieve a similar number of observations within each bin and climate category. We then calculated the ratio of short- to long-term median erosion rates ($R_{S/L}$). We found a negative relationship between $R_{S/L}$ and basin area for each K–G

305 climate zone, except the Cold zone (Fig. 7). Generally, short-term erosion rates are several times higher than long-term rates in small basins, whilst in large basins, long-term rates tend to be more similar or even higher than short-term rates. In addition, long-term erosion rates are positively related to the slope gradient and total relief of the river channels ($R^2 = 0.29$ and 0.24, respectively), whilst for short-term erosion rates, the influences of these topographic parameters are unclear (Fig. 8).
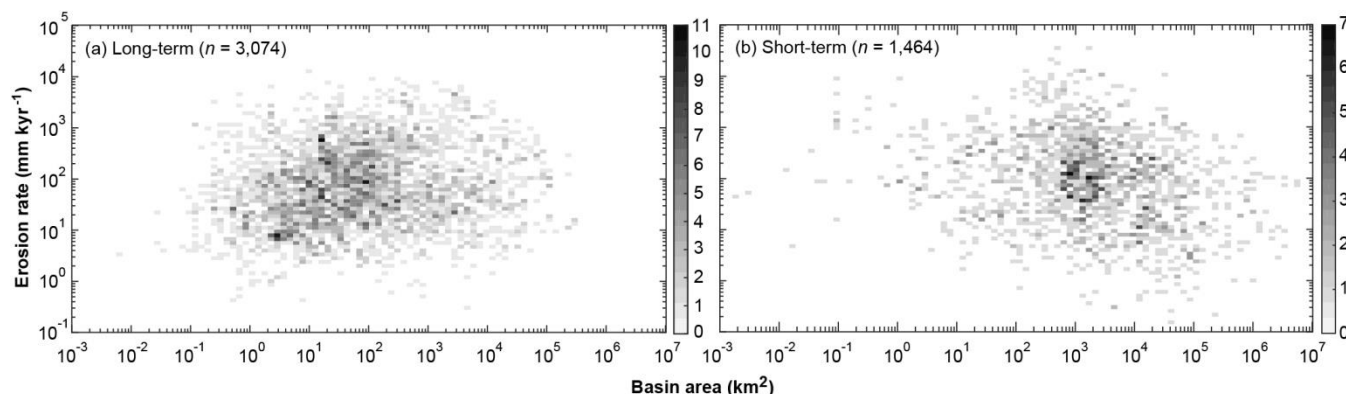
310

Figure 6: The relationships between the drainage basin area and long- (a) and short-term (b) erosion rates. The figures indicate no apparent connection between basin area and either long- or short-term erosion rates.
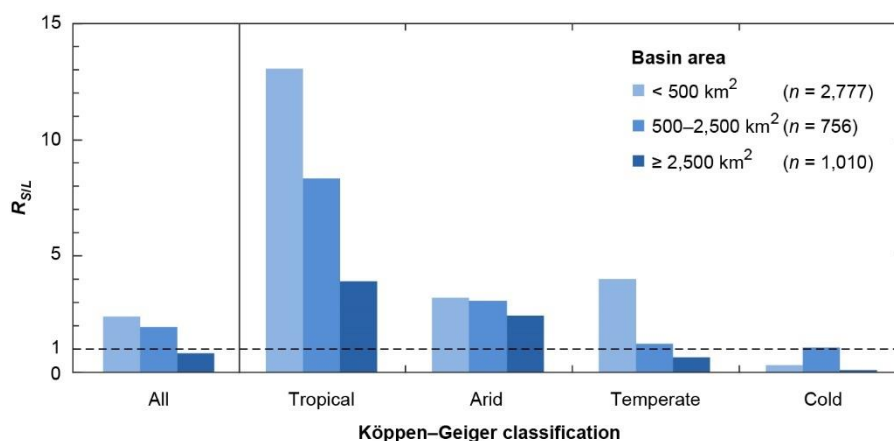

315

Figure 7: The ratio of short- to long-term erosion rates of each basin area bin between climate zones of Köppen–Geiger climate classification. Each ratio was calculated by the medians of short- and long-term erosion rates of each area bin in each climate zone. The numbers of data of each basin area bin (short-term plus long-term erosion rates) are listed in the legend. The dotted lines indicate the same value of short- and long-term rates. Generally, in smaller basins, short-term erosion rates tend to be higher than
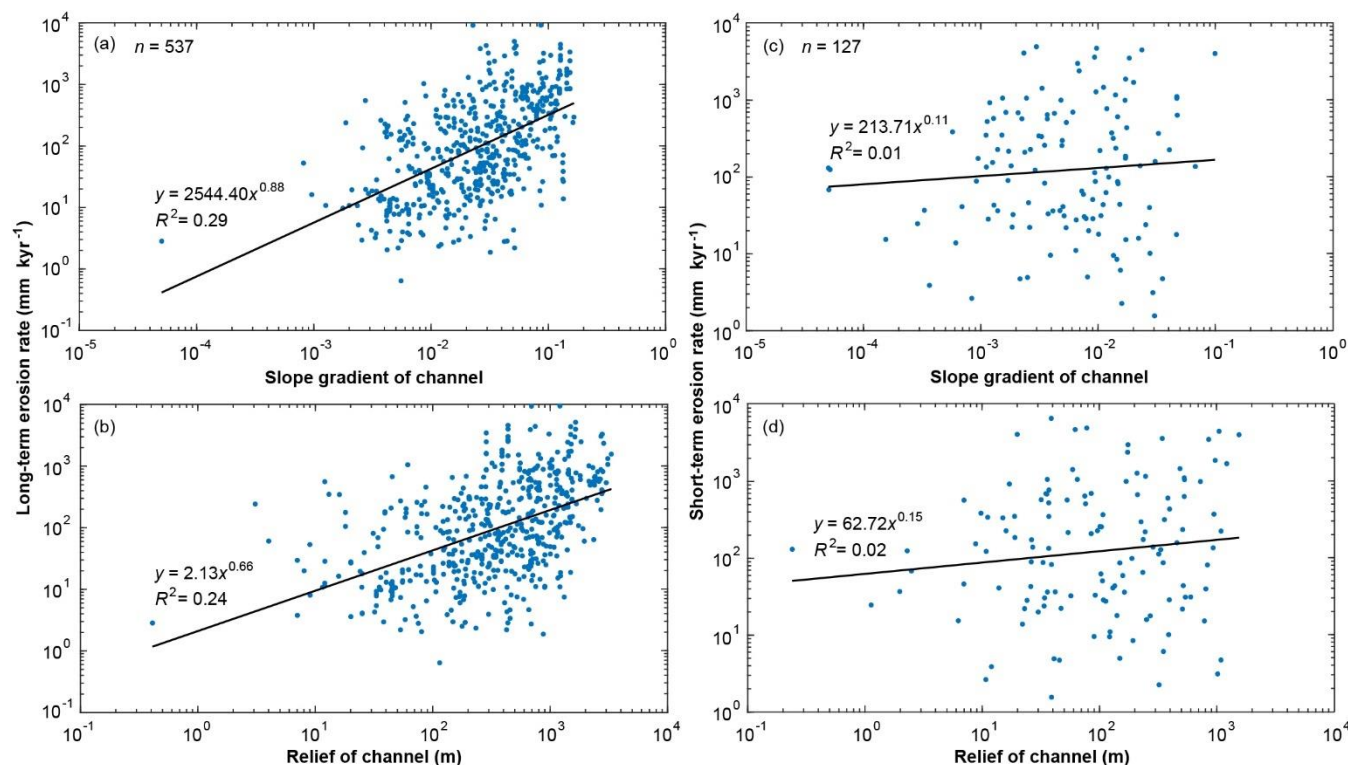320 **long-term rates compared to larger basins.**

Figure 8: The relationships between topographic parameters of river longitudinal profiles and long- (a, b) and short-term (c, d) erosion rates. River profiles were extracted from GLoPro database (Chen et al., 2019) within 150 m of the erosion rate sampling locations. There are positive relationships between long-term erosion rates and channel gradient and relief, whilst the relationships with short-term rates are obscured.

4 Discussion

Drainage basin erosion influences landscape evolution and has been studied widely to estimate its spatial and temporal changes and identify its environmental controls. The dominant controls on erosion rates between locations and over different timescales may vary and climate influence on erosion rates is complex and hard to isolate (Aalto et al., 2006; von Blanckenburg, 2006; Li and Fang, 2016). Climate controls glacial and hydrological processes, which shape the land surface, and it covaries with other factors, such as topography (e.g. orographic precipitation), geology (e.g. weathering and erodibility of lithology), and vegetation cover (Aalto et al., 2006; von Blanckenburg, 2006; Collins and Bras, 2008; Li and Fang, 2016; Chen et al., 2019; Mishra et al., 2019; Sorensen and Yanites, 2019).

Previous studies have shown that, in some regions, short-term erosion rates are higher than long-term rates because of recent human activities (Clapp et al., 2000; Gellis et al., 2004; von Blanckenburg, 2006; Kemp et al., 2020) or climatic change

(Clapp et al., 2000; Gellis et al., 2004; Bierman et al., 2005; Wittmann et al., 2011). In contrast, other regions show higher
340   long-term erosion rates, which were interpreted to be a result of the result of incorporating more high-magnitude, low-
frequency, events (e.g. wildfires, landslides), but are not detectable within short erosion records (Kirchner et al., 2001;
Schaller et al., 2001; Covault et al., 2013). Signals are further complicated by spatial variations of erosion rates within basins
that may not be detected at the basin outlet due to the buffering capacity associated with sediment sequestration along
channels and behind dams, which is more common in large basins (Milliman and Syvitski, 1992; Walling and Fang, 2003;
345   Wilkinson and McElroy, 2007; Wittmann et al., 2011).

Here we compiled long- and short-term drainage basin erosion rates around the globe and analysed the relationships between
erosion rates and potential climatic and environmental controls. We demonstrated that precipitation, former glacial processes,
and topography influence long-term erosion rates, whilst anthropogenic activities dominate short-term erosion rates. In
350   addition, drainage basin area influences the difference between short- and long-term erosion rates, as does aridity.

4.1 Influence of climate on long-term erosion rates

A key finding from this meta-analysis using a large, globally distributed dataset, is that there is a non-linear relationship
between long-term erosion rates and climate (Fig. 3a) which broadly corroborates early theoretical work on short-term
erosion rates (Fig. 9; Langbein and Schumm, 1958; Walling and Kleo, 1979) and subsequent modelling work (Collins and
355   Bras, 2008). Our result is based on a robust scatterplot smoothing method (LOWESS). Based on a small number of data
points, Langbein and Schumm (1958) proposed that sediment yields (as a proxy for erosion rates) in the USA peak in semi-
arid regions due to the combination of rainfall (high enough) and vegetation cover (low enough) that results in optimum
conditions for erosion (Fig. 9). Following their work, Walling and Kleo (1979) analysed sediment yields from around the
globe and in regions with higher humidity. Their result shows that in addition to semi-arid regions, there are also peaks in
360   sediment yield in humid climates, where the precipitation is subject to highly seasonal variability (Fig. 9). These previous
studies can be considered useful theoretical frameworks for interpreting erosion–climate relationships as the data points are
limited and the curves fitted are subjective. Mishra et al. (2019), broadly corroborated this result with compiled global [10]Be
data by showing a non-linear relationship between long-term erosion rate and precipitation which, however, differs in its
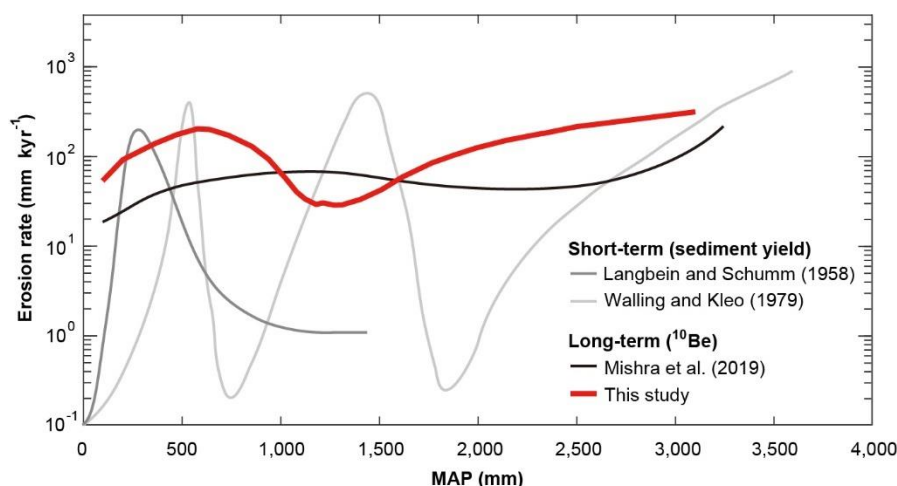peaks and dips relative to the others (Fig. 9).

365

Figure 9: Synthesis of studies showing non-linear relationships between MAP and short-term erosion rates (Langbein and Schumm, 1958, and Walling and Kleo, 1979), and between MAP and long-term erosion rate (Mishra et al., 2019) and this study. See main text for the detailed explanation.

370

Using 3,074 data points, our study shows that there is a relationship between climate and erosion rates that likely results from the interplay between rainfall and vegetation cover (Langbein and Schumm, 1958; Walling and Kleo, 1979; Mishra et al., 2019). Our results show a peak in erosion rates in the Dry sub-humid regions (MAP ~ 600 mm), a dip in the humid regions (MAP ~ 1,250 mm) and then an increase in erosion rates again in the very humid regions (MAP > 1,300 mm). The

375 patterns in Fig. 3a support with an extensive dataset the idea that the interplay between rainfall and vegetation represent an important expression of climate that controls erosion rates globally. In arid regions, rainfall is too low to induce any significant erosion despite the lack of vegetation cover (Molnar et al., 2006). In dry sub-humid regions, the rainfall is high enough and the vegetation cover low enough to result in high erosion rates. In humid regions, the substantive vegetation cover hinders the effectiveness of high precipitation, but as rainfall continues to increase, the highly erosive energy of

380 precipitation exceeds the protective capability of vegetation and results in higher erosion rates again (Collins and Bras, 2008). One major finding of our study is that the systematic relationship between erosion and climate only holds for long-term erosion rates (Fig. 3a), and not for short-term rates (Fig. 3b). We propose that this difference is due to the overwhelming influence of anthropogenic activities on the land surface that masks the inherent climatic influence.

4.2 Influence of glaciation on long-term erosion rates

385 Prior studies argued that in mid- and high-latitude regions, long-term erosion rates tend to be higher than low-latitude regions because glacial processes during ice ages stripped away the underlying land surface and increased physical weathering through freeze–thaw processes (Schaller et al., 2002; Portenga and Bierman, 2011; Harel et al., 2016; Cook et al., 2020). These processes would yield young exposure ages directly after glacial retreat, after which the rates might not be expected to change much in the absence of glacial processes. Since cosmogenic radionuclide-derived erosion rates span the

390   period of glaciation up to the present, they average over the relatively fast and high erosion by glaciers and the subsequent low erosion period. We quantified the role of glaciers in producing such high long-term erosion rates through our comparison of formerly glaciated versus non-glaciated areas within temperate regions (Fig. 4). This analysis showed five times higher erosion rates for the formerly glaciated locations within the same Temperate K–G climate zone, which is consistent with previous studies (Schaller et al., 2002; Portenga and Bierman, 2011; Harel et al., 2016). This result is

395   consistent with the relatively low ratio of short- to long-term erosion for the Humid AI category (Fig. 2b), which likely arises in part because the Humid class includes 46% of the total number of formerly glaciated sites included in our analysis. Overall, our results suggest that post-glacial erosion rates within temperate areas were much lower due to widespread vegetation cover and thick soils, and the long-term average mostly reflects the result of glacial erosion.

4.3 Anthropogenic influence on short-term erosion rates

400   Human activities have increased short-term erosion rates by an estimated one to two orders of magnitude (Milliman and Syvitski, 1992; Dedkov and Mozzherin, 1996; Montgomery, 2007; Wilkinson and McElroy, 2007; Kemp et al., 2020), suggesting that human influences on sediment yields outweigh natural processes (Hooke, 2000; Wilkinson and McElroy, 2007; Kemp et al., 2020). Among the many human activities expressed on surface erosion around the globe, agriculture has one of the highest impacts on the land surface because it directly alters both vegetation through replacement of forest

405   canopies with low-interception coverage crops, and soils through replacement of natural profiles containing developed organic layers with homogenised profiles that undergo cycles of tillage and surface compaction (Hooke, 2000). This anthropogenic disruption of vegetation and soils should create higher susceptibility to erosion by rainsplash, runoff, and wind (Dedkov and Mozzherin, 1996; Wilkinson and McElroy, 2007; Kemp et al., 2020). The eroded material would then contribute to stream channels, where it would be measured as elevated sediment flux compared to pre-historic levels.

410

Our analysis showed that short-term erosion rates are higher than the long-term rates in all climate categories, except for the K–G Cold zone (Fig. 2). The short-term erosion rates within this zone, mainly concentrated in Canada, Eastern Europe, and Russia, are significantly lower than other climate zones (Fig. 2a, Table 1), which we suggest is because most of these regions are covered by contiguous boreal forest that protects the land surface from erosion. Moreover, once we classified short-term

415   erosion rates by land-use categories, we found that erosion in croplands and pastures and rangelands is similar, but these rates are significantly higher than erosion rates for classes without anthropogenic influences (Fig. 5). These results demonstrate that human activities significantly increase short-term erosion rates, that they are consistently detectable around the globe, and that these influences outweigh natural controls including climate and topography (Fig. 2, 3b, 8c, d, Table 1). We note that short-term erosion rates are likely to change in the future due to both changes in human land use and due to the

420   regional expression of climate change. For example, milder winters and less snow cover in higher latitudes may promote more land management activities such as forestry, agriculture, and road building, all of which could rapidly increase short-term erosion rates (Serreze et al., 2000). Even though the prevailing agriculture types between climate zones are different

and may have different impacts on erosion, our results strongly point to the overwhelming impact of agriculture and related activities on short-term erosion rates, corroborating previous work (Dedkov and Mozzherin, 1996; Montgomery, 2007;

425 Wilkinson and McElroy, 2007; Kemp et al., 2020).

However, it is worth noting that the difference in short-term erosion rates between anthropogenic and non-anthropogenic regions shown here is smaller than was shown in previous studies (Dedkov and Mozzherin, 1996; Montgomery, 2007; Wilkinson and McElroy, 2007; Kemp et al., 2020). For example, Dedkov and Mozzherin (1996) estimated that

430 anthropogenic activities increase sediment yields by a factor of 3.5 in large rivers and 8 in small rivers. We speculate that one of the main reasons for this discrepancy is that here we may be underestimating the amount of area that is influenced by anthropogenic activity, based on our defined threshold of > 50% agricultural area. Another possibility is that our analysis may be including more short-term erosion rates sampled in anthropogenically impacted regions, where substantial soil and water conservation efforts in upstream basins, as well as engineering structures (e.g. dams) that trap sediment may result in

435 artificially lower sediment yields (Walling and Webb, 1996; Hooke, 2000; Walling and Fang, 2003; Syvitski et al., 2005; Wilkinson and McElroy, 2007; Singer and Dunne, 2006; Singer and Aalto, 2009).

4.4 Physiographic controls on basin-averaged erosion rates

Although drainage basin area is commonly used (in combination with slope) as a proxy for erosion (i.e. stream power incision law), we found no clear relationship between basin area and long-term or short-term erosion rates within our

440 compiled global dataset (Fig. 6), consistent with other studies (e.g. Summerfield and Hulton, 1994; Kirchner et al., 2001; DiBiase et al., 2010). There are several factors that potentially obscure any systematic relationship between basin area and erosion including sampling location within the basin, tectonic setting, and underlying lithology. Cosmogenic radionuclide-derived erosion rates assume a uniform average erosion rate within the upstream contributing area, so sampling location matters. Samples taken in lower order streams (upper parts of basins) reflect more hillslope and debris flow erosion (Stock

445 and Dietrich, 2003), whereas downstream samples reflect more fluvial erosion, but may be biased by floodplain storage of sediment, violating the detachment-limited assumption within area–erosion relationships (Whipple et al., 1999). Tectonic setting controls the topographic relief of the basin, where active margins have higher relief and steepness than passive margins, promoting higher erosion rates and lower deposition (Ahnert, 1984; Milliman and Meade, 1983; Walling and Webb, 1996; Whipple et al., 1999). Underlying lithology also affects erosion rates, yielding lower exhumation for basins with

450 harder basement rocks for the same drainage area (Hurst et al., 2013). Finally, climate influences the development of soils and vegetation cover, as well as orographic gradients, all of which in turn affect erosion, irrespective of basin area (Dedkov and Mozzherin, 1996; Walling and Webb, 1996; Willett, 1999; Collins and Bras, 2010; Milliman and Farnsworth, 2011).

When we classified erosion rates by basin area, we found a negative relationship between $R_{S/L}$ (the ratio of short- to long-

455 term erosion rates) and basin area for each of the Köppen–Geiger climate zones, except the Cold zone (Fig. 7). Studies have

shown that in large basins (e.g. Amazon River), the differences between long- and short-term erosion rates are less discernible compared to small basins, due to the sediment buffering capacity of large drainage basins (Wittmann et al., 2011; Covault et al., 2013). Buffering capacity, or the degree of sediment transport delay from the source area to the basin outlet in response to the variations of environmental controls, is determined by the balance between sediment supply (affected by

460 erosion rate and river transport capacity) and the accommodation of deposition, such as riverbed or flood plain (Wittmann et al., 2011; Covault et al., 2013). Large basins usually have higher buffering capacity, since they tend to have longer river channels and larger flood plains; therefore, short-term variations of sediment supply from the uplands may be diluted within the basin (i.e. the increased sediments may deposit temporarily when transported along the river channel), and harder to be detected at the downstream sections (Jerolmack and Paola, 2010).

465

The $R_{S/L}$ values are insensitive to basin area within Arid catchments (Fig. 7). We argue that this is because arid regions have a distinctive hydrological regime, where storms tend to have shorter duration, smaller spatial coverage, and high spatial variability, which generate partial area runoff (Yair et al., 1978; Singer and Michaelides, 2017; Michaelides et al., 2018). Arid regions also experience transmission losses within porous river channels, resulting in a breakdown in the relationship

470 between basin area and streamflow, compared to the positive relationship found in humid regions (Knighton and Nanson, 1997; Tooth, 2000; Jaeger et al., 2017; Singer and Michaelides, 2014). These characteristic features of arid zone hydrology reduce the influence of basin area on hydrological processes, including sediment transportation, leading to weaker influence of buffering capacity of drainage basins in arid regions. In the Temperature and Cold zones, the $R_{S/L}$ values are generally lower than the other two categories (i.e. long-term erosion rates are more similar to short-term rates, or even higher) because

475 glacial processes during past ice ages led to increased long-term rates (Section 4.2). In addition to glacial processes, wildfires, landslides and volcanic events that exhibit high magnitude and low frequency, may also lead to higher long-term erosion rates in humid climate zones (Kirchner et al., 2001; Schaller et al., 2001; Covault et al., 2013) as the higher soil coverage can generate large amounts of sediment. The rarity of these large magnitude events means that they are not usually captured in short-term records. The increased timescale of [10]Be-derived erosion rates provides a higher probability that extreme erosion

480 events are included in the data record.

Drainage basin steepness is considered a critical control on erosion rates (e.g. Summerfield and Hulton, 1994; Granger et al., 1996; Portenga and Bierman, 2011), which is also fundamental to the stream power incision law. Drainage basins with higher steepness tend to produce higher velocity of runoff because of the downslope vector of potential energy, which

485 increase the shear stress of water flow and thus produce higher erosion that shapes land surface and transports sediments downstream (Knighton, 1998; Whipple and Tucker, 1999). In addition, steep drainage basins are often located in tectonic-active regions, with low strength of bedrock (because of joints and faults developments), high frequency of landslides (Binnie et al., 2007; Grin et al., 2018), and high precipitation rates caused by orographic effects (Willett, 1999; Roe et al., 2002), all of which would tend to increase erosion rates. Our analyses show positive relationships between slope gradient

490 and total relief of river channels and long-term erosion rates (Fig. 8a, b), suggesting that both climatic and topographic factors control long-term erosion rates despite no clear relationship between short-term erosion rates and these topographic controls (Fig. 8c, d). Short-term erosion rates are dominated by anthropogenic activities. Agriculture, a key anthropogenic influence on erosion, tends to cluster in downstream parts of drainage basins with gentler slopes (Wilkinson and McElroy, 2007). In upstream sections of drainage basins, anthropogenic activities that accelerate erosion (e.g. deforestation) may be

495 ameliorated (from a sediment yield perspective) by soil and water conservation efforts (Montgomery, 2007), and/or by the trapping of sediment within reservoirs (Walling and Webb, 1996; Walling and Fang, 2003; Syvitski et al., 2005). Thus, sediment yields may differ substantially from upstream to downstream within the same basin, depending on the locations of these anthropogenic activities within the landscape. Therefore, human-induced sediment yields may generate unclear relationships between short-term erosion rates and steepness of drainage basins.

5 Conclusions

By compiling and analysing erosion rates from globally distributed sites, we demonstrate a few key differences in long- and short-term rates and their dominant controls: 1) short-term erosion rates are significantly higher than long-term erosion rates in all climate zones except in the K–G Cold zone; 2) long-term erosion rates are higher in mid- and high-latitude regions (and in K–G Cold zone), which were enhanced by glacial processes during past ice ages; 3) only long-term erosion rates are

505 strongly related to climate and topography, while short-term rates do not exhibit any relationship to climatic or topographic factors; 4) short-term rates seem to be dominated by human activities which mask natural controls; 5) a key finding is that a non-linear relationship exists between long-term erosion rates and climate, reflecting the balance between precipitation and vegetation cover; however, this relationship does not hold for the short-term erosion rates as proposed by former studies (Langbein and Schumm, 1958; Walling and Kleo, 1979); 6) short-term erosion rates are generally several times higher than

510 long-term rates in small basins, showing that human-induced erosion is more detectable in small basins with lower sediment buffering capacity; 7) on the contrary, long-term erosion rates tend to be similar or even higher than short-term rates in large basins. The latter can be explained by former glacial processes and high-magnitude, low frequency natural events such as wildfires, mass movements, and volcanic activity (Kirchner et al., 2001; Schaller et al., 2001; Covault et al., 2013). Based on these findings we suggest that erosion rates around the world, regardless of climate zone, are likely to change in the future in

515 response to both climate change and anthropogenic influences, which are growing in prevalence globally.

Data availability.

Short-term erosion rate data are available at the University of Bristol data repository, data.bris, at https://doi.org/10.5523/bris.1pq50eh0902da25aps5nhc1ngv.

Earth **Surface**
Dynamics
Discussions
Open Access
EGU

Author contribution.

520 All authors contributed to the design and interpretation of the study. S.-A.C. carried out data collection and analyses. S.-A.C. wrote the manuscript with invaluable assistance from the co-authors.

Competing interests.

The authors declare that they have no conflict of interest.

References

525 Aalto, R., Dunne, T., and Guyot, J. L.: Geomorphic controls on Andean denudation rates, J. Geol., 114, 85–99, https://doi.org/10.1086/498101, 2006.

Ahnert, F.: Local relief and the height limits of mountain ranges, Am. J. Sci., 284, 1035–1055, https://doi.org/10.2475/ajs.284.9.1035, 1984.

Asner, G. P., Elmore, A. J., Olander, L. P., Martin, R. E., and Harris, A. T.: Grazing systems, ecosystem responses, and
530 global change, Annu. Rev. Environ. Resour., 29, 261–299, https://doi.org/10.1146/annurev.energy.29.062403.102142, 2004.

Bierman, P. R., and Caffee, M.: Slow rates of rock surface erosion and sediment production across the Namib Desert and escarpment, southern Africa, Am. J. Sci., 301, 326–358, https://doi.org/10.2475/ajs.301.4-5.326, 2001.

Bierman, P. R., Reuter, J. M., Pavich, M., Gellis, A. C., Caffee, M. W., and Larsen, J.: Using cosmogenic nuclides to
535 contrast rates of erosion and sediment yield in a semi-arid, arroyo-dominated landscape, Rio Puerco Basin, New Mexico, Earth Surf. Process. Landf., 30, 935–953, https://doi.org/10.1002/esp.1255, 2005.

Binnie, S. A., Phillips, W. M., Summerfield, M. A., and Fifield, L. K.: Tectonic uplift, threshold hillslopes, and denudation rates in a developing mountain range, Geology, 35, 743–746, https://doi.org/10.1130/G23641A.1, 2007.

Brown, E. T., Stallard, R. F., Larsen, M. C., Raisbeck, G. M., and Yiou, F.: Denudation rates determined from the
540 accumulation of in situ-produced ^{10}Be in the Luquillo Experimental Forest, Puerto Rico, Earth Planet. Sci. Lett., 129, 193–202, https://doi.org/10.1016/0012-821X(94)00249-X, 1995.

Cannon, S. H., Powers, P. S., and Savage, W. Z.: Fire-related hyperconcentrated and debris flows on Storm King Mountain, Glenwood Springs, Colorado, USA, Environ. Geol., 35, 210–218, https://doi.org/10.1007/s002540050307, 1998.

Chen, S.-A., Michaelides, K., Grieve, S. W. D., and Singer, M. B.: Aridity is expressed in river topography globally, Nature,
545 573, 573–577, https://doi.org/10.1038/s41586-019-1558-8, 2019.

Clapp, E. M., Bierman, P. R., Schick, A. P., Lekach, J., Enzel, Y., and Caffee, M.: Sediment yield exceeds sediment production in arid region drainage basins, Geology, 28, 995–998, https://doi.org/10.1130/0091-7613(2000)28<995:SYESPI>2.0.CO;2, 2000.

Clapp, E. M., Bierman, P. R., Nichols, K. K., Pavich, M., and Caffee, M.: Rates of sediment supply to arroyos from upland
550   erosion determined using in situ produced cosmogenic ^{10}Be and ^{26}Al, Quat. Res., 55, 235–245,
https://doi.org/10.1006/qres.2000.2211, 2001.

Codilean, A. T., Fenton, C. R., Fabel, D., Bishop, P., and Xu, S.: Discordance between cosmogenic nuclide concentrations in
amalgamated sands and individual fluvial pebbles in an arid zone catchment, Quat. Geochronol., 19, 173–180,
https://doi.org/10.1016/j.quageo.2012.04.007, 2014.

555   Codilean, A. T., Munack, H., Cohen, T. J., Saktura, W. M., Gray, A. G., and Mudd, S. M.: OCTOPUS: an open cosmogenic
isotope and luminescence database, Earth Syst. Sci. Data, 10, 2123–2139, https://doi.org/10.5194/essd-10-2123-2018,
2018.

Collins, D. B. G., and Bras, R. L.: Climatic control of sediment yield in dry lands following climate and land cover change,
Water Resour. Res., 44, W10405, https://doi.org/10.1029/2007WR006474, 2008.

560   Collins, D. B. G., and Bras, R. L.: Climatic and ecological controls of equilibrium drainage density, relief, and channel
concavity in dry lands, Water Resour. Res., 46, W04508, https://doi.org/10.1029/2009WR008615, 2010.

Cook, S. J., Swift, D. A., Kirkbride, M. P., Knight, P. G., and Waller, R. I.: The empirical basis for modelling glacial erosion
rates, Nat. Commun., 11, 759, https://doi.org/10.1038/s41467-020-14583-8, 2020.

Covault, J. A., Craddock, W. H., Romans, B. W., Fildani, A., and Gosai, M.: Spatial and temporal variations in landscape
565   evolution: historic and longer-term sediment flux through global catchments, J. Geol., 121, 35–56,
https://doi.org/10.1086/668680, 2013.

Dedkov, A. P., and Mozzherin, V. I.: Erosion and sediment yield on the Earth, in: Erosion and Sediment Yield: Global and
Regional Perspectives, edited by: Walling, D. E., and Webb, B. W., IAHS Publications, Wallingford, Oxfordshire, UK,
236, 29–36, 1996.

570   DiBiase, R. A., Whipple, K. X., Heimsath, A. M., and Ouimet, W. B.: Landscape form and millennial erosion rates in the
San Gabriel Mountains, CA, Earth Planet. Sci. Lett., 289, 134–144, https://doi.org/10.1016/j.epsl.2009.10.036, 2010.

Dosseto, A., and Schaller, M.: The erosion response to Quaternary climate change quantified using uranium isotopes and in
situ-produced cosmogenic nuclides, Earth-Sci. Rev., 155, 60–81, https://doi.org/10.1016/j.earscirev.2016.01.015, 2016.

Dunne, T., and Leopold, L. B.: Water in Environmental Planning, Freeman, New York, US, 1978.

575   Foley, J. A., DeFries, R., Asner, G. P., Barford, C., Bonan, G., Carpenter, S. R., Chapin, F. S., Coe, M. T., Daily, G. C., and
Gibbs, H. K.: Global consequences of land use, Science, 309, 570–574, https://doi.org/10.1126/science.1111772, 2005.

Gellis, A. C., Pavich, M. J., Bierman, P. R., Clapp, E. M., Ellevein, A., and Aby, S.: Modern sediment yield compared to
geologic rates of sediment production in a semi-arid basin, New Mexico: assessing the human impact, Earth Surf. Process.
Landf., 29, 1359–1372, https://doi.org/10.1002/esp.1098, 2004.

580   Granger, D. E., Kirchner, J. W., and Finkel, R.: Spatially averaged long-term erosion rates measured from in situ-produced
cosmogenic nuclides in alluvial sediment, J. Geol., 104, 249–257, https://doi.org/10.1086/629823, 1996.

Granger, D. E., Lifton, N. A., and Willenbring, J. K.: A cosmic trip: 25 years of cosmogenic nuclides in geology, GSA Bull., 125, 1379–1402, https://doi.org/10.1130/B30774.1, 2013.

Granger, D. E., and Schaller, M.: Cosmogenic nuclides and erosion at the watershed scale, Elements, 10, 369–373,
585   https://doi.org/10.2113/gselements.10.5.369, 2014.

Grin, E., Schaller, M., and Ehlers, T. A.: Spatial distribution of cosmogenic ^{10}Be derived denudation rates between the Western Tian Shan and Northern Pamir, Tajikistan, Geomorphology, 321, 1–15, https://doi.org/10.1016/j.geomorph.2018.08.007, 2018.

Han, Y., An, Z., Marlon, J. R., Bradley, R. S., Zhan, C., Arimoto, R., Sun, Y., Zhou, W., Wu, F., Wang, Q., Burr, G. S., and
590   Cao, J.: Asian inland wildfires driven by glacial–interglacial climate change, Proc. Natl. Acad. Sci., 117, 5184–5189, https://doi.org/10.1073/pnas.1822035117, 2020.

Harel, M.-A., Mudd, S. M., and Attal, M.: Global analysis of the stream power law parameters based on worldwide ^{10}Be denudation rates, Geomorphology, 268, 184–196, https://doi.org/10.1016/j.geomorph.2016.05.035, 2016.

Hilley, G. E., Porder, S., Aron, F., Baden, C. W., Johnstone, S. A., Liu, F., Sare, R., Steelquist, A., and Young, H. H.:
595   Earth's topographic relief potentially limited by an upper bound on channel steepness, Nat. Geosci., 12, 828–832, https://doi.org/10.1038/s41561-019-0442-3, 2019.

Hooke, R. L.: On the history of humans as geomorphic agents, Geology, 28, 843–846, https://doi.org/10.1130/0091-7613(2000)28<843:OTHOHA>2.0.CO;2, 2000.

Hurst, M. D., Mudd, S. M., Yoo, K., Attal, M., and Walcott, R.: Influence of lithology on hillslope morphology and response
600   to tectonic forcing in the northern Sierra Nevada of California, J. Geophys. Res. Earth Surf., 118, 832–851, https://doi.org/10.1002/jgrf.20049, 2013.

Jaeger, K. L., Sutfin, N. A., Tooth, S., Michaelides, K., and Singer, M.: Geomorphology and sediment regimes of intermittent rivers and ephemeral streams, in: Intermittent Rivers and Ephemeral Streams: Ecology and Management, edited by: Datry, T., Bonada, N., and Boulton, A., Elsevier, 21–49, https://doi.org/10.1016/B978-0-12-803835-2.00002-4,
605   2017.

Jerolmack, D. J., and Paola, C.: Shredding of environmental signals by sediment transport, Geophys. Res. Lett., 37, L19401, https://doi.org/10.1029/2010GL044638, 2010.

Kemp, D. B., Sadler, P. M., and Vanacker, V.: The human impact on North American erosion, sediment transfer, and storage in a geologic context, Nat. Commun., 11, 6012, https://doi.org/10.1038/s41467-020-19744-3, 2020.

610   Kirchner, J. W., Finkel, R. C., Riebe, C. S., Granger, D. E., Clayton, J. L., King, J. G., and Megahan, W. F.: Mountain erosion over 10 yr, 10 k.y., and 10 m.y. time scales, Geology, 29, 591–594, https://doi.org/10.1130/0091-7613(2001)029<0591:MEOYKY>2.0.CO;2, 2001.

Knighton, A., and Nanson, G.: Distinctiveness, diversity and uniqueness in arid zone river systems, in: Arid Zone Geomorphology: Process, Form and Change in Drylands, second edition, edited by: Thomas, D. S. G., John Wiley & Sons,
615   Chichester, West Sussex, UK, 185–203, 1997.

Knighton, D.: Fluvial Forms and Processes: A New Perspective, Edward Arnold, London, UK, 1998.

Langbein, W. B., and Schumm, S. A.: Yield of sediment in relation to mean annual precipitation, Eos, Trans. AGU, 39, 1076–1084, https://doi.org/10.1029/TR039i006p01076, 1958.

Laronne, J. B.: Very high rates of bedload sediment transport by ephemeral desert rivers, Nature, 366, 148–150, https://doi.org/10.1038/366148a0, 1993.

Li, Z., and Fang, H.: Impacts of climate change on water erosion: a review, Earth-Sci. Rev., 163, 94–117, https://doi.org/10.1016/j.earscirev.2016.10.004, 2016.

Meyer, G. A., Pierce, J. L., Wood, S. H., and Jull, A. J. T.: Fire, storms, and erosional events in the Idaho batholith, Hydrol. Process., 15, 3025–3038, https://doi.org/10.1002/hyp.389, 2001.

Michaelides, K., Hollings, R., Singer, M. B., Nichols, M. H., and Nearing, M. A.: Spatial and temporal analysis of hillslope–channel coupling and implications for the longitudinal profile in a dryland basin, Earth Surf. Process. Landf., 43, 1608–1621, https://doi.org/10.1002/esp.4340, 2018.

Milliman, J. D., and Meade, R. H.: World-wide delivery of river sediment to the oceans, J. Geol., 91, 1–21, https://doi.org/10.1086/628741, 1983.

Milliman, J. D., and Syvitski, J. P.: Geomorphic/tectonic control of sediment discharge to the ocean: the importance of small mountainous rivers, J. Geol., 100, 525–544, https://doi.org/10.1086/629606, 1992.

Milliman, J. D., and Farnsworth, K. L. (Eds.): River Discharge to the Coastal Ocean: A Global Synthesis, Cambridge University Press, Cambridge, UK, 2011.

Mishra, A. K., Placzek, C., and Jones, R.: Coupled influence of precipitation and vegetation on millennial-scale erosion rates derived from [10]Be, PloS One, 14, e0211325, https://doi.org/10.1371/journal.pone.0211325, 2019.

Molnar, P., Anderson, R. S., Kier, G., and Rose, J.: Relationships among probability distributions of stream discharges in floods, climate, bed load transport, and river incision, J. Geophys. Res. Earth Surf., 111, F02001, https://doi.org/10.1029/2005JF000310, 2006.

Montgomery, D. R.: Soil erosion and agricultural sustainability, Proc. Natl. Acad. Sci., 104, 13268–13272, https://doi.org/10.1073/pnas.0611508104, 2007.

NOAA PSL, Boulder, Colorado, USA, CPC US Unified Precipitation data, https://psl.noaa.gov, last access: 13 January 2020.

Pan, B.-T., Geng, H.-P., Hu, X.-F., Sun, R.-H., and Wang, C.: The topographic controls on the decadal-scale erosion rates in Qilian Shan Mountains, N.W. China, Earth Planet. Sci. Lett., 292, 148–157, https://doi.org/10.1016/j.epsl.2010.01.030, 2010.

Peel, M. C., Finlayson, B. L., and McMahon, T. A.: Updated world map of the Köppen-Geiger climate classification, Hydrol. Earth Syst. Sci. Discuss., 4, 439–473, https://hal.archives-ouvertes.fr/hal-00298818, 2007.

Pierce, J. L., Meyer, G. A., and Jull, A. J. T.: Fire-induced erosion and millennial-scale climate change in northern ponderosa pine forests, Nature, 432, 87–90, https://doi.org/10.1038/nature03058, 2004.

Portenga, E. W., and Bierman, P. R.: Understanding Earth's eroding surface with [10]Be, GSA Today, 21, 4–10,
650   https://doi.org/10.1130/G111A.1, 2011.

Ramankutty, N., and Foley, J. A.: Estimating historical changes in global land cover: Croplands from 1700 to 1992,
        Global Biogeochem. Cycles, 13, 997–1027, https://doi.org/10.1029/1999GB900046, 1999.

Ray, N., and Adams, J.: A GIS-based vegetation map of the world at the Last Glacial Maximum (25,000-15,000 BP),
        Internet Archaeol., 11, https://archive-ouverte.unige.ch/unige:17817, 2001.

655   Roe, G. H., Montgomery, D. R., and Hallet, B.: Effects of orographic precipitation variations on the concavity of steady-state
        river profiles, Geology, 30, 143–146, https://doi.org/10.1130/0091-7613(2002)030<0143:EOOPVO>2.0.CO;2, 2002.

Schaller, M., von Blanckenburg, F., Hovius, N., and Kubik, P.: Large-scale erosion rates from in situ-produced cosmogenic
        nuclides in European river sediments, Earth Planet. Sci. Lett., 188, 441–458, https://doi.org/10.1016/S0012-
        821X(01)00320-X, 2001.

660   Schaller, M., von Blanckenburg, F., Veldkamp, A., Tebbens, L., Hovius, N., and Kubik, P.: A 30 000 yr record of erosion
        rates from cosmogenic [10]Be in Middle European river terraces, Earth Planet. Sci. Lett., 204, 307–320,
        https://doi.org/10.1016/S0012-821X(02)00951-2, 2002.

Schmidt, A. H., Neilson, T. B., Bierman, P. R., Rood, D. H., Ouimet, W. B., and Gonzalez, V. S.: Influence of topography
        and human activity on apparent in situ [10]Be-derived erosion rates in Yunnan, SW China, Earth Surf. Dynam., 4, 819–830,
665   http://dx.doi.org/10.5194/esurf-4-819-2016, 2016.

Serreze, M. C., Walsh, J. E., Chapin III, F. S., Osterkamp, T., Dyurgerov, M., Romanovsky, V., Oechel, W. C., Morison, J.,
        Zhang, T., and Barry, R. G.: Observational evidence of recent change in the northern high-latitude environment, Clim.
        Change, 46, 159–207, https://doi.org/10.1023/A:1005504031923, 2000.

Singer, M. B., and Dunne, T.: Modeling decadal bed material sediment flux based on stochastic hydrology, Water Resour.
670   Res., 40, W03302, https://doi.org/10.1029/2003WR002723, 2004.

Singer, M. B., and Dunne, T.: Modeling the influence of river rehabilitation scenarios on bed material sediment flux in a
        large river over decadal timescales, Water Resour. Res., 42, W12415, https://doi.org/10.1029/2006WR004894, 2006.

Singer, M. B., and Aalto, R.: Floodplain development in an engineered setting, Earth Surf. Process. Landf., 34, 291–304,
        https://doi.org/10.1002/esp.1725, 2009.

675   Singer, M. B., and Michaelides, K.: How is topographic simplicity maintained in ephemeral dryland channels?, Geology, 42,
        1091–1094, https://doi.org/10.1130/G36267.1, 2014.

Singer, M. B., and Michaelides, K.: Deciphering the expression of climate change within the Lower Colorado River basin by
        stochastic simulation of convective rainfall, Environ. Res. Lett., 12, 104011, https://doi.org/10.1088/1748-9326/aa8e50,
        2017.

680   Sorensen, C. S., and Yanites, B. J.: Latitudinal trends in modern fluvial erosional efficiency along the Andes,
        Geomorphology, 329, 170–183, https://doi.org/10.1016/j.geomorph.2018.12.030, 2019.

Stock, J., and Dietrich, W. E.: Valley incision by debris flows: Evidence of a topographic signature, Water Resour. Res., 39, https://doi.org/10.1029/2001WR001057, 2003.

685 Struck, M., Jansen, J. D., Fujioka, T., Codilean, A. T., Fink, D., Fülöp, R.-H., Wilcken, K. M., Price, D. M., Kotevski, S., and Fifield, L. K.: Tracking the ^{10}Be–^{26}Al source-area signal in sediment-routing systems of arid central Australia, Earth Surf. Dynam., 6, 329–349, https://doi.org/10.5194/esurf-6-329-2018, 2018.

Summerfield, M., and Hulton, N.: Natural controls of fluvial denudation rates in major world drainage basins, J. Geophys. Res. Solid Earth., 99, 13871–13883, https://doi.org/10.1029/94JB00715, 1994.

Syvitski, J. P., Vörösmarty, C. J., Kettner, A. J., and Green, P.: Impact of humans on the flux of terrestrial sediment to the

690 global coastal ocean, Science, 308, 376–380, https://doi.org/10.1126/science.1109454, 2005.

Syvitski, J. P., and Milliman, J. D.: Geology, geography, and humans battle for dominance over the delivery of fluvial sediment to the coastal ocean, J. Geol., 115, 1–19, https://doi.org/10.1086/509246, 2007.

Tofelde, S., Duesing, W., Schildgen, T. F., Wickert, A. D., Wittmann, H., Alonso, R. N., and Strecker, M.: Effects of deep-seated versus shallow hillslope processes on cosmogenic ^{10}Be concentrations in fluvial sand and gravel, Earth Surf.

695 Process. Landf., 43, 3086–3098, https://doi.org/10.1002/esp.4471, 2018.

Tooth, S.: Process, form and change in dryland rivers: a review of recent research, Earth Sci. Rev., 51, 67–107, https://doi.org/10.1016/S0012-8252(00)00014-3, 2000.

Trabucco, A., and Zomer, R. J.: Global Aridity and PET Database, CGIAR Consortium for Spatial Information, http://www.cgiar-csi.org/data/global-aridity-and-pet-database, 2009.

700 U.S. Geological Survey, National Water Information System data available on the World Wide Web (USGS Water Data for the Nation): https://waterdata.usgs.gov/nwis, last access: 2 December 2019.

von Blanckenburg, F.: The control mechanisms of erosion and weathering at basin scale from cosmogenic nuclides in river sediment, Earth Planet. Sci. Lett., 237, 462–479, https://doi.org/10.1016/j.epsl.2005.06.030, 2006.

von Blanckenburg, F., and Willenbring, J. K.: Cosmogenic nuclides: dates and rates of Earth-surface change, Elements, 10,

705 341–346, https://doi.org/10.2113/gselements.10.5.341, 2014.

Walling, D., and Webb, B.: Erosion and sediment yield: a global overview, in: Erosion and Sediment Yield: Global and Regional Perspectives, edited by: Walling, D. E., and Webb, B. W., IAHS Publications, Wallingford, Oxfordshire, UK, 236, 3–20, 1996.

Walling, D., and Fang, D.: Recent trends in the suspended sediment loads of the world's rivers, Global Planet. Change, 39,

710 111–126, https://doi.org/10.1016/S0921-8181(03)00020-1, 2003.

Walling, D. E., and Kleo, A. H. A.: Sediment yields of rivers in areas of low precipitation: a global view, in: The Hydrology of Areas of Low Precipitation, IAHS Publications, Wallingford, Oxfordshire, UK, 128, 479–493, 1979.

Whipple, K. X., Kirby, E., and Brocklehurst, S. H.: Geomorphic limits to climate-induced increases in topographic relief, Nature, 401, 39–43, https://doi.org/10.1038/43375, 1999.

715   Whipple, K. X., and Tucker, G. E.: Dynamics of the stream-power river incision model: Implications for height limits of mountain ranges, landscape response timescales, and research needs, J. Geophys. Res. Solid Earth, 104, 17661–17674, https://doi.org/10.1029/1999JB900120, 1999.

Wilkinson, B. H., and McElroy, B. J.: The impact of humans on continental erosion and sedimentation, GSA Bull., 119, 140–156, https://doi.org/10.1130/B25899.1, 2007.

720   Willett, S. D.: Orogeny and orography: The effects of erosion on the structure of mountain belts, J. Geophys. Res. Solid Earth, 104, 28957–28981, https://doi.org/10.1029/1999JB900248, 1999.

Wittmann, H., von Blanckenburg, F., Maurice, L., Guyot, J.-L., Filizola, N., and Kubik, P. W.: Sediment production and delivery in the Amazon River basin quantified by in situ–produced cosmogenic nuclides and recent river loads, GSA Bull., 123, 934–950, https://doi.org/10.1130/B30317.1, 2011.

725   Yair, A., Sharon, D., and Lavee, H.: An instrumented watershed for the study of partial area contribution of runoff in the arid zone, Z. Geomorphol. Suppl., 29, 71–82, 1978.

Yizhou, W., Huiping, Z., Dewen, Z., Wenjun, Z., Zhuqi, Z., Weitao, W., and Jingxing, Y.: Controls on decadal erosion rates in Qilian Shan: re-evaluation and new insights into landscape evolution in north-east Tibet, Geomorphology, 223, 117–128, https://doi.org/10.1016/j.geomorph.2014.07.002, 2014.